AD-A265 716

(2)

:NTATION PAGE

Form Approved
OMB No. 0704-0188

1. AGENCY USE ONLY (Leave blank)	2. REPORT DATE	3. REPORT TYPE AND DATES COVERED
	April 1993	Final Report 01 Mar 89 - 28 Feb 93

4. TITLE AND SUBTITLE

Short Wavelength Crystal Fiber Devices

5. FUNDING NUMBERS

AFOSR-89-0263

6. AUTHOR(S)

Dr N. Djeu

7. PERFORMING ORGANIZATION NAME(S) AND ADDRESS(ES)

Department of Physics
University of South Florida
Tampa FL 33620-57000

8. PERFORMING ORGANIZATION REPORT NUMBER

AFOSR-TR- 93 0393

9. SPONSORING/MONITORING AGENCY NAME(S) AND ADDRESS(ES)

AFOSR/NE
110 Duncan Avenue Suite B115
Bolling AFB DC 20332-0001

10. SPONSORING/MONITORING AGENCY REPORT NUMBER

2301/A1

11. SUPPLEMENTARY NOTES

12a. DISTRIBUTION/AVAILABILITY STATEMENT

UNLIMITED

12b. DISTRIBUTION CODE

13. ABSTRACT *(Maximum 200 words)*

SEE REPORT FOR ABSTRACT

93 6 1 0 4

93-13131

14. SUBJECT TERMS			15. NUMBER OF PAGES
			16. PRICE CODE
17. SECURITY CLASSIFICATION OF REPORT	18. SECURITY CLASSIFICATION OF THIS PAGE	19. SECURITY CLASSIFICATION OF ABSTRACT	20. LIMITATION OF ABSTRACT
UNCLASSIFIED	UNCLASSIFIED	UNCLASSIFIED	UNLIMITED

SHORT WAVELENGTH CRYSTAL FIBER DEVICES

FINAL REPORT
AFOSR-89-0263
APRIL, 1993

Prepared by:

N. Djeu
Department of Physics
University of South Florida
Tampa, FL 33620-5700
(813) 974-2121

The potential of crystal fibers for the generation of short wavelength visible laser radiation was explored under this program. There were two major thrusts to this work. One of them was the search for a suitable technique to produce low loss crystal fibers. Implantation cladding of bare crystal fibers with high energy ion beams was investigated for this purpose. The other was the identification of a suitable upconversion process which would be amenable for implementation in the crystal fiber form. For that the upconversion laser potential of Tm:YAG was explored.

Crystal fibers of a variety of materials have been successfully produced by a number of laboratories around the world, including our own, using the laser heated pedestal growth (LHPG) technique. Typically, the minimum diameter of a fiber that can be grown by this technique is of the order of 30μm. Therefore, ideally the cladding procedure should accomplish two objectives. First, it should significantly reduce the diameter of the core so that the resulting fiber would support only a few modes, if not a single mode. Second, it should allow one to independently vary the refractive index and thickness of the clad region, which is necessary for optimizing the waveguiding properties of the finished fiber given the fact that the starting fiber cannot be made smaller than 30μm.

Ion implantation was selected to convert the outer portion of the crystal fiber into cladding because the method appeared to have all the desired characteristics. To demonstrate the feasibility of the technique $LiNbO_3$ fiber was selected as the prototype material

both because it is readily grown using LHPG and because the effects of ion implantation on $LiNbO_3$ were reasonably well understood. In particular, it was known that up to 2MeV the penetration by He^+ ions varied approximately linearly with energy. Additionally, the index reduction near the end of the range could be controlled by varying the total dosage.

To investigate implantation cladding, a-axis $LiNbO_3$ fibers were grown on the LHPG facility in our own laboratory. To render the fibers optically homogeneous, a procedure was developed to pole the bi-domained as-grown fibers prior to implantation. They were then attached to a heat sink with the use of silver print and taken to the high energy ion beam facility at NRL for implantation. The maximum He^+ beam energy that could be delivered was typically in the 6-7 MeV range. Generally two energies were used in order to build up the thickness of the region with reduced refractive index. To insure good radial symmetry the beam was made to be incident from two orthogonal directions, each making a 45° angle to the heat sink normal. Afterwards the fibers were detached from the heat sink, turned over, and re-attached. The same implantation procedure was then repeated. The implanted fibers were placed inside quartz capillaries with epoxy, and their ends polished for optical characterizations.

Both optical contrast microscopy and index profiling of the polished fiber ends revealed that the ion beam penetrated a distance of nearly 20μm. Propagation measurements at 1.06μm were made on a piece of implanted a-axis $LiNbO_3$ fiber which measured

44μm x 66μm in cross section. The output beam from the 11 mm long fiber was virtually undistorted, and the waveguiding loss was estimated to be 0.3 dB cm^{-1}. Most of this loss is believed to be caused by the optical damage suffered by the $LiNbO_3$. (See Appendix I for further details.) These results establish ion implantation as a promising technique for the cladding of crystal fibers.

In order to demonstrate a short wavelength crystal fiber device a suitable upconversion system must be identified. Preliminary measurements in our laboratory indicated that Tm:YAG is an efficient upconverter from the red/near IR to the blue. Furthermore, studies by others showed that the desired index modification by ion implantation is also possible in YAG. A two pronged approach was taken to determine the feasibility of such a crystal fiber device. On the one hand upconversion laser experiments in bulk Tm:YAG were undertaken to assess if processes such as excited state absorption could be a problem. These experiments led to the first upconversion laser ever in an oxide crystal. The laser worked only at cryogenic temperatures since the effective gain length in the bulk crystal was only about 1 mm. However, spontaneous emission measurements indicated that a room temperature laser should be possible in a fiber several centimeters in length if waveguiding loss can be made sufficiently low. (See Appendix II).

In the meantime implantation cladding studies in YAG were also conducted. Unfortunately, contrary to expectation, no apparent index modification was observed. This was tentatively attributed to

the fact that our implantation was done at room temperature and not 77K as by other workers. The lower temperature was not used out of the fear that the fragile fiber bonded to the heat sink would not survive the temperature cycling. The high cost of accessing the ion beam facility at NRL precluded further attempts to find out whether our fears were well founded, and if so whether alternate methods of heat sinking the fibers could be developed.

In conclusion, the results obtained under this program indicate that implantation cladding is a viable approach to the production of low loss crystal fibers. We also demonstrated for the first time an upconversion laser in an oxide crystal. This is important since fluorides are easily destroyed by the implantation process. Future work in this area should focus on the development of a cryogenic fiber implantation technology and on the investigation of other potential oxide upconversion hosts.

APPENDIX I

a reprint from Optics Letters

Cladding of a crystal fiber by high-energy ion implantation

D. P. S. Saini, Y. Shimoji, R. S. F. Chang, and N. Djeu

Department of Physics, University of South Florida, Tampa, Florida 33620-5700

Received January 28, 1991

The feasibility of using a multi-MeV He^+-ion beam to convert the outer portion of a crystal fiber into cladding is demonstrated. When applied to *a*-axis $LiNbO_3$ fiber, the resulting structure has been found to show good waveguiding characteristics.

Because of their ability to confine light waves to small transverse dimensions over long distances, optical fibers have proved themselves to be highly useful for the implementation of laser and nonlinear-optical devices as well as amplifiers. Thus far nearly all such devices have been based on glass fibers. The development of crystal fiber fabrication techniques to expand the family of materials available for such applications is clearly of interest. Organic crystal fibers have indeed been prepared by growth in capillary tubes, while high-quality inorganic crystal fibers have been grown by the laser-heated pedestal-growth (LHPG) technique.[1] Optoelectronic devices in both types of crystal fiber have been demonstrated, but so far only in rudimentary forms.[2,3]

The LHPG technique is capable of producing a large variety of crystal fibers. In practice, however, one can only grow fibers as small as approximately 30 μm in cross section with this technique. This severely inhibits the full exploitation of these fibers for the intended applications. For doped crystal fibers outdiffusion has been shown to be a feasible technique for converting the outer portion of the fiber into a cladding.[4] The application of this technique, however, appears to be rather limited. For undoped crystal fibers, indiffusion has been tried as a means to produce a smaller core, but the result was not completely satisfactory.[5] In this Letter we report the results of an investigation in which ion implantation was used to produce a cladding in a crystal fiber.

For this feasibility study $LiNbO_3$ was selected, since the optical effects of ion implantation on this material are reasonably well understood.[6] The LHPG system used to grow the $LiNbO_3$ fibers has been described elsewhere.[7] Since we were interested in using the fibers ultimately in frequency-doubling experiments, they were grown along the *a* axis of the crystal. Optical-quality, single-crystal $LiNbO_3$ was used as the starting material. The initial feed had a circular cross section and measured just under 1 mm in diameter. Fibers with cross sections of the order of 50 μm were obtained after two diameter-reduction steps on the LHPG system.

Earlier studies of *a*-axis $LiNbO_3$ fibers grown by the LHPG technique have shown them to be bidomained with the domain wall parallel to the *c* face.[8] The fibers therefore had to be poled with the following procedure. Two *a*-axis $LiNbO_3$ fibers were placed between polished $LiNbO_3$ plates with their domain walls parallel to the surfaces of the plates. The plates together with the fibers were then placed in a tube furnace. The temperature of the furnace was raised to 1020–1100°C at a rate of 2°C/min. As the maximum temperature was reached, a dc voltage of 15 V was applied across the plates. It was left on as the entire assembly was cooled down to room temperature at a rate of 1°C/min. The use of $LiNbO_3$ plates as electrodes prevented any material loss of the fibers at the high temperatures. The poled fibers were polished lengthwise in the *y* face for domain structure observations. It was found that complete poling was achieved when the maximum temperature exceeded 1020°C.

The poled $LiNbO_3$ fiber was attached with silver paint to a stainless-steel heat sink in preparation for ion implantation. The fiber was positioned with its *c* face parallel to the heat-sink surface. When the proper thickness of paint was used, it was possible to attach the fiber without having the paint creep up its sides. The fiber was then implanted by a He^+ beam from two directions, each 45° from the normal to the heat-sink surface. The ion-beam had a 3-mm diameter and was scanned along the 2-cm length of the fiber. At each angle, two ion beam energies were used, 6 and 5.5 MeV, in that order. The implantation dosage at each energy was 5×10^{15} ions cm^{-2}. The reason for using two ion energies was that earlier research had shown that at a given He^+ energy the region of reduced refractive index was peaked with a width of approximately 1 μm at the stopping range of the ions, which varied approximately linearly with the ion energy.[6] Thus two ion energies were used with the intention of broadening the width of that region to minimize leakage of the resulting waveguide modes. After implantation from the two directions, the fiber was removed from the heat sink with a solvent, turned 180° around, and reattached. Then the same procedure was applied to the other side.

The implanted fiber was placed in a glass capillary tube with epoxy. A few millimeters of each end was

0146-9592/91/141074-03$5.00/0

Fig. 1. Transmission micrograph of He^+-ion-implanted a-axis $LiNbO_3$ fiber. The cross section of the fiber is defined by the outer boundary of the optically damaged (dark) region. The line in the lower right is the inner wall of the capillary tube in which the fiber is epoxied.

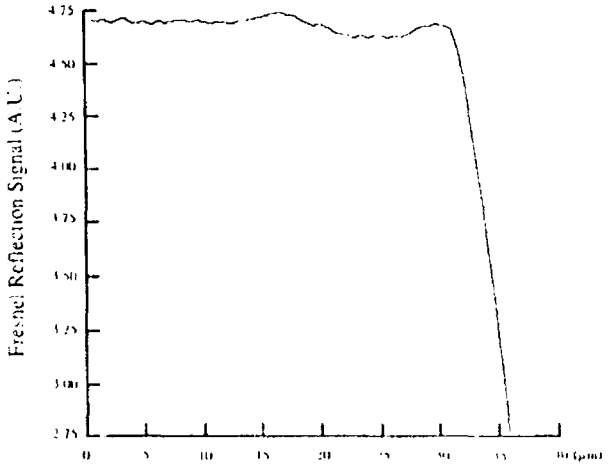

Fig. 2. Fresnel reflection signal in arbitrary units for half the fiber along the y axis in mid-plane. Zero on the horizontal axis corresponds to the center of the fiber, and the sharp falloff at 33 μm corresponds to the edge of the fiber. The core–cladding boundary occurs between 15 and 20 μm. The resolution is approximately 2 μm.

sawed off, and the ends were then polished to give a net fiber length of 11 mm. A micrograph of the fiber cross section taken in transmission is shown in Fig. 1. The outer perimeter of the dark portion defines the cross-sectional appearance of the a-axis $LiNbO_3$ fiber. It has the same shape as that observed by Luh *et al.*, a distorted oval with two growth ridges at opposite ends of one of the diagonals.[8] One of the ridges is visible in the lower left-hand corner of the fiber shown in Fig. 1, while the other one in the upper right-hand corner was apparently chipped off during polishing. The fiber measured 44 μm in the short dimension (the c axis) and 66 μm in the long dimension (the y axis). Implantation is seen to have produced optical damage to a depth of as much as 20 μm at some points, leaving a sharply defined unpenetrated core region.

The refractive-index profile of the implanted fiber was probed by measuring the Fresnel reflection of a focused 632.8-nm He–Ne laser beam. The laser beam was linearly polarized with its field parallel to the y axis of the fiber and had a diameter of 2 μm in the beam waist. Figure 2 shows the Fresnel reflection signal when the beam was scanned from the center of the fiber out to the edge along its long dimension. It is seen that near the surface of the fiber the refractive index is essentially the same as that of the unaltered core, which was also found to be the case at lower He^+ energies.[6] This is followed by a region of lower refractive index, again in agreement with earlier findings. Then the index rises to a value greater than that of the core just before the ions reach the end of their range. This increase was not explicitly indicated in earlier research, although one would draw that conclusion from an extrapolation of the reported results. A comparison of Figs. 1 and 2 shows that the boundary of the optically damaged region corresponds to the peak in the Fresnel reflection signal. Using the relationship $\Delta R/R = 4n(\Delta n/n)/(n^2 - 1)$, where R is the reflectivity and n is the index of refraction, one calculates $\Delta n_0 = 0.05$ for the index difference between the peak and the core region and $\Delta n_0 = -0.09$ for that between the valley and the core region at 632.8 nm.

The waveguiding characteristics of the fiber were investigated with a cw Nd:YAG laser, which was also linearly polarized along the y axis of the crystal. The best output from the fiber in terms of power and spatial uniformity was obtained when an elliptically shaped beam measuring 18 μm × 27 μm in the beam waist was used as the input. The intensity profiles along the major and minor axes of the beam in the far field measured 12 cm from the output end of the fiber with a diode array are shown in Fig. 3. Except for the two side lobes in the direction parallel to the long dimension of the fiber, the beam was essentially the lowest-order elliptical Gaussian. The throughput of the fiber under these conditions was 70% after correction for the Fresnel losses at the two ends. To estimate the loss associated with the waveguide itself, the fiber was shortened to 8 mm, and the transmission measurement was repeated. The throughput was found to improve by approximately 2%, which implied a coupling efficiency of 77% and a waveguide loss of 0.3 dB cm^{-1}.

Second-harmonic generation in the implantation-clad fiber was attempted with a pulsed Nd:glass laser that was tunable from 1060 to 1083 nm.

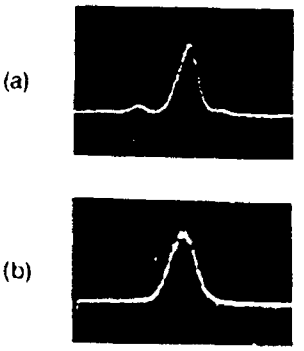

Fig. 3. Spatial profile of the 1.06-μm beam after propagation through the implanted fiber, measured 12 cm from the output end, (a) parallel and (b) perpendicular to the long dimension (the y axis) of the fiber. The FWHM is (a) 2.3 mm and (b) 3.1 mm.

When the laser beam was focused to a circular spot with a diameter of approximately 10 μm on the fiber, the second-harmonic component of the output from the fiber was readily detected. It peaked at 1086 nm and amounted to a few microwatts for an input peak power of the order of 1 W. Since the 1-μm output from the fiber was highly multimode with this coupling, we believe that second-harmonic generation took place in a short distance near the input end without the benefit of waveguiding. As the phase-matching wavelength of the starting material was 1072 nm, the unusually long phase-matching wavelength observed was probably caused by the loss of Li in the fiber growth process.[9] When optimal coupling with a 18 μm × 27 μm elliptical beam was used, no green output was observed anywhere within the tuning range of the laser. Apparently phase matching has been shifted for the waveguide modes to wavelengths longer than 1088 nm.

In conclusion, we have demonstrated that ion implantation is a feasible way to convert the outer portion of a crystal fiber into a cladding. In the case of a-axis $LiNbO_3$ fiber, in spite of the odd shape of the cross section, reasonably low-loss guided-wave propagation has been obtained in such a structure. Since most of the ionic crystals studied thus far show a decrease in the refractive index as a result of amorphization caused by ion implantation,[6] this may prove to be a general technique for the cladding of crystal fibers. Furthermore, it should be possible to produce cores of the order of a few micrometers by starting with smaller fibers or implanting with higher-energy ion beams.

We thank B. P. Scott for his assistance in the operation of the tunable Nd:glass laser. This research was supported by the U.S. Air Force Office of Scientific Research and the Defense Advanced Research Projects Agency.

References

1. M. M. Fejer, J. L. Nightingale, G. A. Magel, and R. L. Byer, Rev. Sci. Instrum. **55**, 1791 (1984).
2. P. Kerkoc, C. Bosshard, H. Arend, and P. Gunter, Appl. Phys. Lett. **54**, 487 (1989).
3. M. J. F. Digonnet, C. J. Gaeta, D. O'Meara, and H. J. Shaw, IEEE J. Lightwave Technol. **LT-5**, 642 (1987).
4. C. A. Burrus and L. A. Coldren, Appl. Phys. Lett. **31**, 383 (1977).
5. S. Sudo, A. Cordova-Plaza, R. L. Byer, and H. J. Shaw, Opt. Lett. **12**, 938 (1987).
6. P. D. Townsend, Rep. Prog. Phys. **50**, 501 (1987).
7. R. S. F. Chang, S. Sengupta, G. J. Dixon, L. B. Shaw, and N. Djeu, Proc. Soc. Photo-Opt. Instrum. Eng. **1104**, 244 (1989).
8. Y. S. Luh, R. S. Feigelson, M. M. Fejer, and R. L. Byer, J. Cryst. Growth **78**, 135 (1986).
9. J. G. Bergman, A. Ashkin, A. A. Ballman, J. M. Dziedzic, H. J. Levinstein, and R. G. Smith, Appl. Phys. Lett. **12**, 92 (1968).

APPENDIX II

Upconversion-pumped blue laser in Tm:YAG

B. P. Scott, F. Zhao, R. S. F. Chang, and N. Djeu

Department of Physics, University of South Florida, Tampa, Florida 33620

Received July 15, 1992

We have demonstrated an upconversion-pumped blue laser on the $^1G_4$–$^3H_6$ band of Tm:YAG at cryogenic temperatures. Measurements were also made to assess the possibility of room-temperature upconversion-pumped lasers in Tm:YAG on both the $^1G_4$–$^3H_6$ and the $^1D_2$–$^3F_4$ bands.

The upconversion-pumped blue Tm^{3+} laser on the $^1G_4$–$^3H_6$ band was first demonstrated in $YLiF_4$ by Hebert *et al.*[1] Subsequently, lasers operating on the same band were reported in ZBLAN fiber and in $BaY_{1.0}Yb_{0.99}F_8$.[2,3] Most recently, room-temperature cw operation in ZBLAN fiber was obtained by pumping in the 1.1-μm region.[4] We report here what is to our knowledge the first upconversion-pumped blue Tm^{3+} laser on the $^1G_4$–$^3H_6$ band in an oxide crystal. While low temperature is required for the operation of this laser in bulk YAG crystal, we present data that suggest that room-temperature operation in this crystal should be possible in guided-wave structures.

The upconversion pumping scheme used to make the blue Tm:YAG laser is shown in Fig. 1. A photon at 785 nm excites the Tm^{3+} ion to the $^3H_4$ level. The Tm^{3+} ion then cross relaxes by interacting with a neighboring ground-state ion to yield two ions in the metastable $^1F_4$ level. A second photon at 638 nm subsequently pumps the $^3F_4$ ion to the $^1G_4$ upper laser level. This is believed to be the dominant pumping mechanism for the laser reported here, although other excitation channels are also operative, as is discussed below.

The laser was fabricated from a Tm:YAG crystal with 3% doping. It measured 1 mm × 1 mm × 3 mm and had reflectors with 1-cm radius of curvature put on the ends. The pump end reflected >99.9% at 485 nm and transmitted 73% and >90% at 638 and 785 nm, respectively, whereas the output end reflected 99.5% at 485 nm. The crystal was mounted in a cryostat capable of reaching temperatures as low as 10 K. The 785- and 638-nm pumps were provided by a Ti:sapphire laser and a dye laser. The output from each laser was expanded and collimated to a diameter of 7 mm. The two beams were then combined and focused into the crystal with a 12.5-cm focal-length lens. The output from the Ti:sapphire laser was nearly diffraction limited, whereas the dye laser beam was approximately 1.5 times diffraction limited.

The spontaneous blue emission from the excitation region observed through a polished side of the crystal was spectrally analyzed. At a starting heat-sink temperature of 10 K and maximum pump powers of 340 mW at 785 nm and 190 mW at 638 nm, the strongest features were identified as transitions from the lowest Stark component of the $^1G_4$ manifold to the Z_3, Z_4, and Z_5 components of the ground manifold, using the designations of Gruber *et al.*[5] The blue emission disappeared almost completely when the dye laser beam was blocked but remained at nearly half the intensity when the Ti:sapphire laser beam was blocked. The strong excitation that was achieved with dye laser pumping alone at 638 nm can be explained by the absorption avalanche process, in which absorption builds up from a low initial level through accumulation of ions in the metastable state.[6]

When the pump beams were correctly aligned with respect to the crystal, laser threshold was reached with 340 mW at 785 nm and 100 mW at 638 nm. The laser wavelength was found to be 486.2 nm, corresponding to the transition terminating in the Z_4 component of the $^3H_6$ ground manifold that lies 241 cm^{-1} above the lowest Stark component. Measurement with a photodiode showed that the output

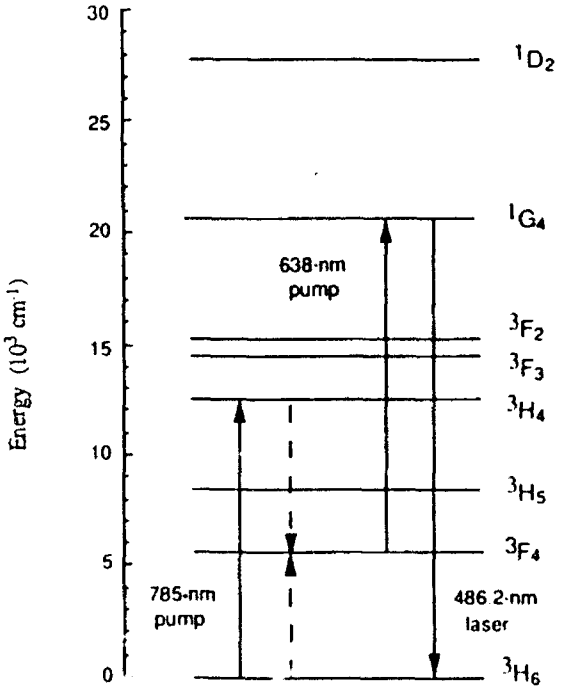

Fig. 1. Dominant pumping mechanism for the blue upconversion laser in Tm:YAG.

0146-9592/93/020113-03$5.00/0

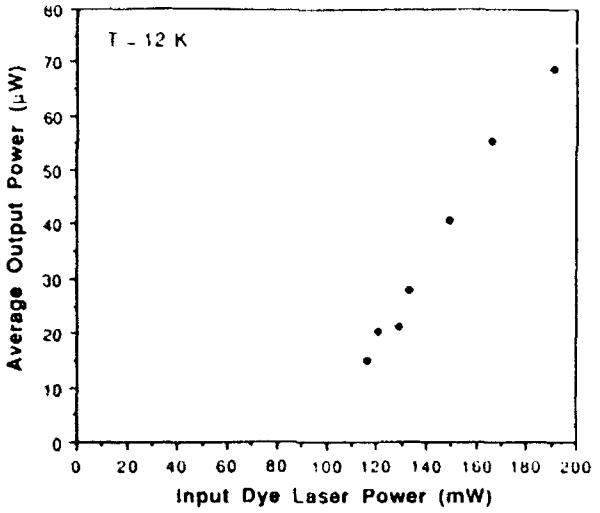

Fig. 2. Average blue laser power versus dye laser pump power. The Ti:sapphire laser incident power was 340 mW.

consisted of a train of 14-ns pulses. While there was considerable jitter in the pulse repetition rate, the individual pulses were quite constant in both shape and amplitude. As the laser was taken above threshold by increasing the dye laser power, the main effect was a shortening of the interpulse time. The individual pulses remained essentially the same. The variation of the average blue laser power with incident dye laser power is shown in Fig. 2. From the average power, the pulse repetition rate, and the pulse shape, the peak power of the pulses was determined to be 15 W. The effect of temperature on the laser was also investigated. At maximum pump powers, laser output decreased steadily with increasing temperature. The highest temperature at which laser output was observed was 30 K.

We believe that the pulsing behavior of the laser output resulted from passive Q switching caused by either self-absorption or excited-state absorption. Because the pump beams were tightly focused into the crystal, the spot sizes near the ends were significantly larger than those in the focal region. Near the pump mirror end there was maximum power deposition by the Ti:sapphire beam. The heat-sink temperature was observed to rise by 2 K when the Ti:sapphire beam was incident on the crystal. The local temperature rise in the pumped region near the pump mirror end might have been much larger. At the same time, upconversion pumping in this area was weak because of the large spot sizes. Thus, the laser transition could well have been uninverted in that region. Alternatively, there could have been excited-state absorption from the $^3F_4$ level to the $^1I_6$ level, because one of the components in that transition has been calculated to overlap the laser line to within 1 cm^{-1}.[5] The passive Q-switching explanation is supported by the fact that the measured spontaneous emission on the blue band was approximately two orders of magnitude larger than the maximum average laser power extracted.

To assess the feasibility of extending the operation of the upconversion blue Tm:YAG laser to higher temperatures, side-light emission measurements at room temperature were made. For these measurements the input lens was changed to one having a focal length of 8.8 cm, and the crystal was pumped with only the dye laser beam, which was spatially filtered. Furthermore, only emission from a region contained well within the Rayleigh range of the beam focus in the crystal was monitored. It was found that at room temperature the optimal dye laser wavelength for upconversion pumping shifts from 638 to 647 nm. The dependence of the emitted power for the $^1G_4 - ^3H_6$ band on dye laser intensity at 647 nm is shown in Fig. 3. The dye laser intensity in the beam waist was calculated from the incident power after we corrected for transmission through the pump mirror, assuming that there were no beam distortion effects present. The emitted power shows a threshold similar to that observed in Tm:$YAlO_3$ at room temperature, although its value is approximately an order of magnitude higher than in YALO.[7] Furthermore, as we show below, in the case of Tm:YAG more than one avalanche absorption process may have contributed to the excitation of the high-lying levels. It should be noted that even at the highest dye laser power available the blue emission was still increasing linearly.

The spectrum of the emission at the highest excitation level is shown in Fig. 4. A comparison with the known energy levels of Tm:YAG leads to the identification of the features to the red of 463 nm as belonging to the $^1G_4 - ^3H_6$ band and those to the blue as belonging to the $^1D_2 - ^3F_4$ band. The $^1D_2$ level could have been excited either through direct avalanche absorption from the $^3H_4$ level or through avalanche absorption from $^3F_4$ followed by upconversion involving the $(^1G_4, ^3F_4)$ pair. The relative importance of the two processes cannot be determined with the limited data that we have at hand. We next

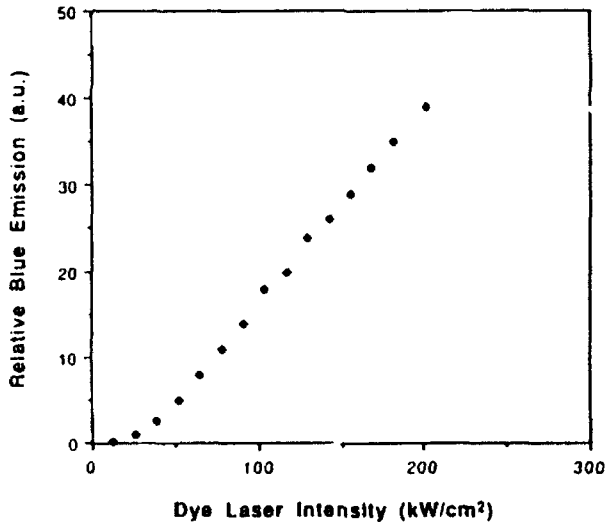

Fig. 3. Room-temperature side-light emission on the $^1G_4 - ^3H_6$ band with dye laser pumping at 647 nm. The intensity given corresponds to that at the peak of the profile. The incident power was 120 mW at maximum intensity.

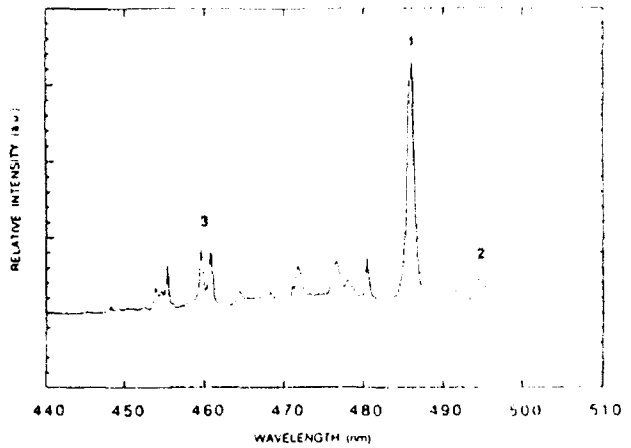

Fig. 4. Room-temperature side-light emission spectrum, uncorrected for detection system response. The detection system was 33% more sensitive at 450 nm than at 500 nm, with an approximately linear variation in between.

evaluate the room-temperature laser potential of both the $^1G_4-{}^3H_6$ and the $^1D_2-{}^3F_4$ bands in Tm:YAG.

To assess the gain that could be achieved on the most prominent peaks in the two bands of interest, absolute side-light emission measurements were made. With the assumption that excitation was uniform and contained entirely within the $1/e^2$ radius of the pump beam, the absolute emission data together with the emission spectrum provided an estimate of the gain on the various components. For peak 1 in Fig. 4, which is made up of transitions terminating on Stark components lying between 216 and 247 cm^{-1} above ground, the gain corresponding to maximum pumping in Fig. 3 is estimated to be 0.06 cm^{-1}, assuming negligible population in the lower level. This is a promising peak if ground manifold depletion can be achieved, because excited-state absorption out of the $^3F_3$ level should be negligible at room temperature as a result of multiphonon relaxation. Another prospective laser peak is peak 2 in Fig. 4, which terminates in Stark levels lying more than 588 cm^{-1} above ground. While the estimated gain under the same assumptions is reduced to approximately 0.01 cm^{-1}, ground manifold depletion should not be necessary for this peak. In the $^1D_2-{}^1F_4$ band the most promising features are the doublets labeled 3, which terminate in Stark levels lying more than 550 cm^{-1} above the bottom of the $^1F_4$ manifold. By using the same assumptions again, we find an estimated gain of just over 0.01 cm^{-1} for these peaks. However, excited-state absorption out of $^3H_4$ could be a problem for these transitions.

Gains higher than those estimated above should be achievable for pump intensities greater than the maximum value employed in our studies. The implementation of room-temperature blue upconversion lasers in Tm:YAG would require the use of guided-wave structures, so that high-intensity pumping can be achieved over extended lengths. Waveguide Nd:YAG lasers have been demonstrated in both fiber and channel forms.[8,9] Therefore, in principle, Tm:YAG guided-wave structures can also be produced. Finally, more favorable upconversion dynamics and spectral distributions may be found for the same systems in other host crystals, and their investigations would be worthwhile.

This research was supported by the U.S. Air Force Office of Scientific Research under grant AFOSR-89-0263.

References

1. T. Hebert, R. Wannemacher, R. M. Macfarlane, and W. Lenth, Appl. Phys. Lett. **60**, 2592 (1992).
2. J. Y. Allain, M. Monerie, and H. Poignant, Electron. Lett. **26**, 166 (1990).
3. R. J. Thrash and L. F. Johnson, in *Digest of Conference on Compact Blue-Green Lasers* (Optical Society of America, Washington, D.C., 1992), paper ThB3.
4. S. G. Grubb, K. W. Bennett, R. S. Cannon, and W. F. Humer, Electron. Lett. **28**, 1243 (1992).
5. J. B. Gruber, M. E. Hills, R. M. MacFarlane, C. A. Morrison, G. A. Turner, G. J. Quarles, G. J. Kintz, and L. Esterowitz, Phys. Rev. B **40**, 9464 (1989).
6. J. Chivian, W. Case, and D. Eden, Appl. Phys. Lett. **35**, 124 (1979).
7. H. Ni and S. C. Rand, Opt. Lett. **16**, 1424 (1991).
8. J. L. Nightingale and R. L. Byer, Opt. Lett. **11**, 437 (1986).
9. A. C. Large, S. J. Field, D. C. Hanna, D. P. Shepherd, A. C. Tropper, P. J. Chandler, P. D. Townsend, and L. Zhang, in *Digest of Conference on Lasers and Electro-Optics* (Optical Society of America, Washington, D.C., 1992), paper CWE1.